# ANALYSIS OF GREEN WOOD CHIP FORMATION MECHANISMS AT HIGH CUTTING SPEED

**Renaud Pfeiffer[1], Hubert Maigre[2], Robert Collet[1], Louis Denaud[1], Guillaume Pot[1]**

[1] Arts et Metiers-ParisTech, LaBoMaP (EA 3633) Rue Porte de Paris, 71250 CLUNY-FRANCE
renaud.pfeiffer@ensam.eu, robert.collet@ensam.eu, louis.denaud@ensam.eu, guillaume.pot@ensam.eu
[2] INSA Lyon, LaMCoS, 18-20 rue des Sciences, 69621 VILLEURBANNE-FRANCE
hubert.maigre@insa-lyon.fr

## ABSTRACT

During the primary transformation in wood industry, logs are faced with conical rough milling cutters commonly named slabber or canter heads. Chips produced consist of raw materials for pulp paper and particleboard industries. The process efficiency of these industries partly comes from particle size distribution. However, chips formation is greatly dependent on milling conditions and material variability.
Thus, this study aims at better understanding and predicting chips production in wood milling.
The different mechanisms of their formation are studied through orthogonal cutting experiments at high cutting speed. Chipping observations are carried out on a Chardin's pendulum. This experimental setup, similar to a Charpy's pendulum, was designed to measure cutting forces in sawing. A piezoelectric force transducer records the cutting forces. It is synchronized with a high speed camera to observe the formation of chips. In this experimental campaign, wood specimens are machined with fresh and saturated beech and Douglas fir.
Within these conditions, ejection of free water inside wood can be observed during fragmentation, particularly on saturated beech. As previously seen in quasi-static experiments, chip thickness is proportional to the nominal cut thickness. Moreover, the grain orientation has a great influence on the cutting mechanisms, so as the nominal cut and the grow circles widths. Digital image correlation is carried out in order to observe the strains fields during the cut for different cutting mechanisms.
This chip fragmentation study finally allows the improvement of the cutting conditions in rough milling for slabber manufacturers.

**Keywords:** Slabber, green wood, chip, fragmentation, digital image correlation.

## INTRODUCTION

The aim of sawmills consist in valorising the maximum volume of wood from logs during the primary transformation. After cross cutting and debarking, logs are squared by slabber heads (called canter heads too). During this operation, up to 30 % of the logs initial volume is transformed into chips. These chips are mainly used as raw materials in pulp industries or as fuel. The chip size distribution has a great influence on efficiency in pulp industries and must be controlled.
However the chip dimensions depend on many kinematic, geometric and material parameters. From a macroscopic point of view, many authors (1-3) used industrial canter to produce chips. They observed the influence of macroscopic parameters like feed or log positioning on chip size distribution by screening.

Another approach (4, 5) is to design specifically an experimental setup to observe the fragmentation near the cutting edge. Through this way measurement of cutting forces and strain fields becomes possible. However the cutting speed remains very low (a few $mm.s^{-1}$).
So as to offer a better understanding of the physical chipping processes, this paper focuses on the observation of fragmentation phenomena at usual cutting speed by the use of high speed camera and digital image correlation.

## MATERIALS AND METHODS

### Experimental setup

Chipping experiments are carried out on a Chardin's pendulum, similar to a Charpy's pendulum, but designed to measure cutting energy in sawing (6). Later this equipment is further instrumented with a piezoelectric force sensor to measure cutting forces on dry wood (7). The arm of the pendulum is 1.2 m long and weighs 36 kg. The available kinematic energy thus reaches 756 J and the cutting speed 400 m/min at the impact. The knife used here comes from a CT600 slabber head from LBL-BRENTA-CD with a bevel angle of 40° and a cutting angle of 45°. The specimens with a length of 140 mm are carefully machined on a CNC milling machine to avoid damages on the cut surface.
For this study, additional sensors with respect to (8) are inserted. A displacement laser sensor Keyence LK-H082 is used to measure the cutting length and the variation of the cutting speed along the cut. A Brüel & Kjær 4188 microphone records the sounds produced by the cut. A Brüel & Kjær 4397 accelerometer, located at the extremity of the knife, records the vibrations due to chipping. Like in (7, 8) a Kistler 9257A piezoelectric force sensor records the cutting forces. All the outputs are synchronised and sampled at 50 kHz. The disposition of all these sensors can be seen in Figure 1.
A high speed camera Phantom v9.1 is used to film the cut (maximal resolution 324 x 312 pixels at 50 kHz for cutting experiments and 512 x 640 pixels at 20 kHz for cutting experiments with digital image correlation). Two LED projectors are used to diminish the exposure time to 7 µs. The disposition of video equipment is represented in Figure 2. The camera is trigged with the laser sensor by the way of an Arduino Uno board. The delay caused by the Arduino board is measured and taken into account in the signals synchronisations.
Finally the graduated dial of the pendulum is used to measure the energy dissipated in the cut.

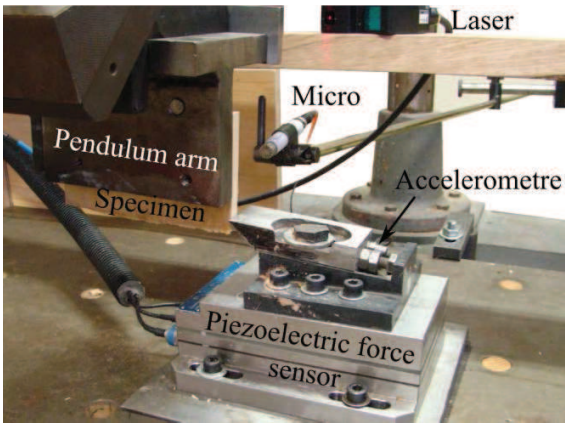


**Figure 1:** Sensors used in the chipping experiments.

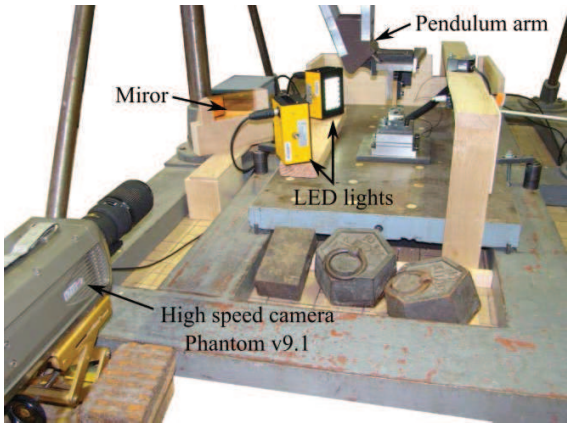


**Figure 2:** Equipment used for chipping movies.

## Experimental method

The aim of this study is to analyse the effect of species, moisture content *MC*, cutting thickness *h* (see (8)), and grain direction angle *GD* on chipping and on cutting energy. The grain direction angle *GD* is defined as the angle between the resultant cutting direction (see (8)) and the wood grain direction.

Two species are selected: beech for its homogeneity and Douglas fir, strongly used in French sawmills but known for its heterogeneity and hard machinability. Just after sawing, fresh slabs of this two species are separated in two groups. One part is wrapped with plastic and put into fridge. Moisture content is determined by double weight technic (MC = 60 % for beech and 40 for Douglas fir). The second part is immerged into water during four months. The day of the experiments, moisture content reaches 130 % for beech and 115 % for Douglas fir.

Two experimental setups are built. The factors of the first one are the cutting thickness *h* and the moisture content for the two species. Due to limited energy capacity of the pendulum, three cutting thicknesses are chosen: 5, 10 and 15 mm. The cutting width *b* stays at 10 mm and the grain direction angle *GD* at 90°. The factors of the second one are the grain direction angle and the moisture content for the two species. In order to observe the transition between chipping and tearing, the grain direction angles chosen are 70, 80, 100 and 110°. The cutting width *b* stays at 10 mm and the cutting thickness at 10 mm too.

Each kind of experiments is repeated six times for a total of 288 experiments.

# RESULTS AND DISCUSSION

## Good chipping areas

Through the analysis of the chips produced and the chipping movies, we are able to define good and bad chipping areas, functions of the grain direction angle *GD*, the moisture content MC and the cutting thickness *h*. An example of chip evolution is shown on Figure 3 for Douglas fir at *h* = 10 mm.

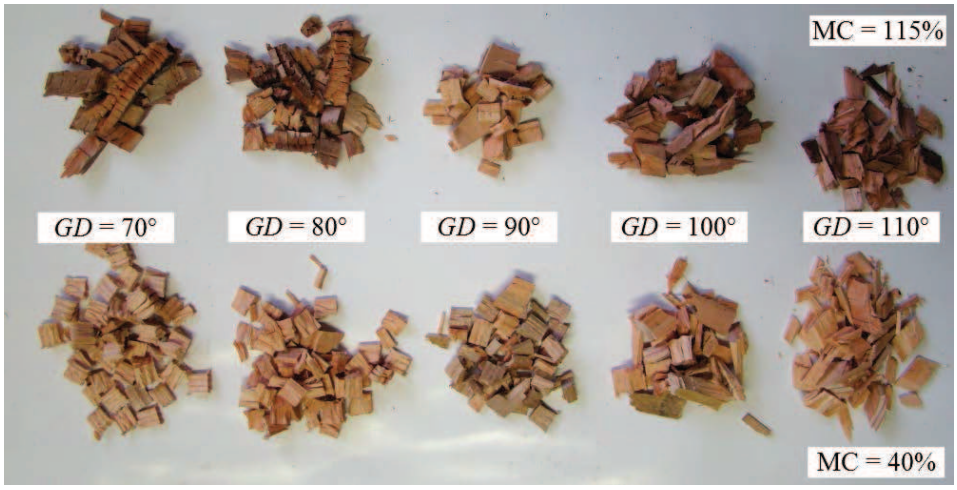


**Figure 3:** Effect of grain angle direction *GD* and moisture content MC on chip geometry. (Douglas fir, *h* = 10 mm, *b* = 10 mm)

For Douglas fir, when $GD \leq 80°$ and for $GD = 90°$ at MC = 40 %, chipping occurs. At a moisture content of 115 % when $GD \leq 80°$, some chips are not completely separated. Although chips impact the knife holder and piezoelectric force sensor after cutting, they are still linked by a few fibres. At this scale of cutting thickness, chipping occurs at the cutting edge. The contact length between chips and knife does not exceed 10 mm so chip breaker is not required.
When *GD* is greater than 90° there is no chip production. Wood shears between growth rings. This effect is only caused by the few growth rings in the specimen thickness. From an energetic point of view, it is easier to shear between growth rings than chipping at cross grain.
For MC = 115 % and *GD* = 90°, a transition state between chipping and separating wood by tearing appears.
At $h = 15$ mm and $GD = 90°$, there is shearing between growth rings too.
For beech at $GD = 110°$ and $h = 10$ mm, no chips are produced but wood is separated by tearing.
For the other values of *GD* and *h*, chipping occurs. Non-fully separated chips can be observed when *GD* is lower than 90°.
From these results the good chipping areas for the two species are plotted in Figures 4 and 5.

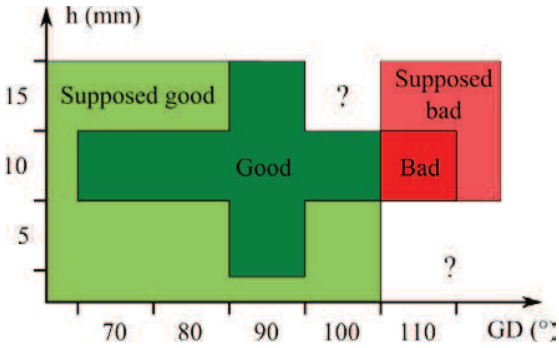


**Figure 4:** Good and bad chipping areas for beech (MC = 60 and 130 %, $b = 10$ mm).

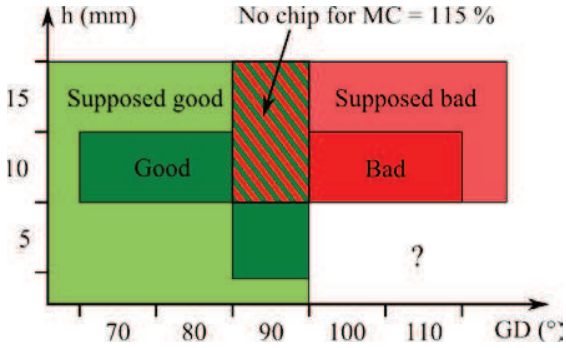


**Figure 5:** Good and bad chipping areas for Douglas fir (MC = 40 and 115 %, $b = 10$ mm).

## Chip thickness and ejection speed

By calibrating the chipping movies, it is possible to measure the chip thickness and the ejection speed of the chips for all the experiments in the movies. These movies have a 107 µm.pixel$^{-1}$ resolution and a 50 kHz frame rate.
Analysing of all the chip thickness - ejection speed couples provides no correlation between them in a similar set of parameters.
For each set of values, when the chipping is well established, 100 chips are drawn on all the repetitions. The area in these well-established conditions corresponds to the 80 mm directly following the first 20 mm after the impact area. Because after these 80 mm, in some conditions the specimen completely splits.
As already mentioned in the literature (1, 2, 4), the chip thickness is proportional to the cutting thickness (Figure 6 and Table 1). Except for the Douglas fir at $h = 10$ mm, the standard deviation increases with the cutting thickness too. To improve the study, a variance analysis (ANOVA) is performed for beech. The chosen model is the following:

$$Y(A,B) = M + E_A.[A] + E_B.[B] + [B]^T.I_{AB}.[A]$$

With:

- $Y$: the observed parameter (here the chip thickness),
- $M$: the global average,
- $E_A$: the effect matrix of factor A (the moisture content),
- $E_B$: the effect matrix of factor B (the cutting thickness),
- $I_{AB}$: the interaction matrix of factors A and B,
- $[A]$: the weight matrix of factor A,
- $[B]$: the weight matrix of factor B.

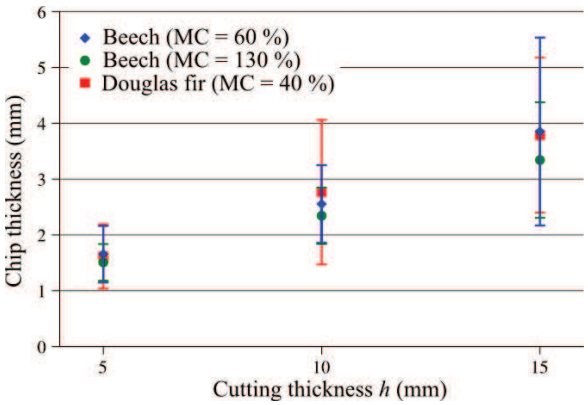


**Figure 6:** Chip thickness function of cutting thickness. Mean and standard deviation of 100 values. ($b$ = 10 mm, $GD$ = 90°)

| Species | MC (%) | Slope | Origin (mm) | $R^2$ |
|---|---|---|---|---|
| Beech | 60 | 0.22 | 0.49 | 0.40 |
| Beech | 130 | 0.18 | 0.56 | 0.54 |
| Douglas fir | 40 | 0.21 | 0.67 | 0.34 |

**Table 1:** Linear regression parameters of the influence of cutting thickness on chip thickness.

The ANOVA shows that moisture content is significant at 1% and has a decreasing effect on chip thickness. Cutting thickness is significant at 1% too and has an increasing effect on chip thickness. However the interaction between these two parameters seems negligible. The details of the factor matrix are visible on Equations 1-4.

$$\boldsymbol{M = 2.54} \qquad \boldsymbol{E_B = [-0.961 \quad -0.094 \quad 1.055]}$$

$$\boldsymbol{E_A = [0.145 \quad -0.145]} \qquad \boldsymbol{I_{AB} = \begin{bmatrix} -0.071 & 0.071 \\ -0.040 & 0.040 \\ 0.110 & -0.110 \end{bmatrix}}$$

**Equations 1-4:** Factor matrix for the chip thickness

At first sight, species, moisture constant and cutting thickness have no influence on ejection speed at GD = 90°. It remains constant at 21 $m.s^{-1}$ (see Figure 7). A variance analysis is carried out with the same parameters as before. It shows that the moisture content is significant at 1% and has an increasing effect on ejection speed while cutting thickness is significant at 5%. Its effect is much more complex because the interaction between these two factors is important at 1% with a high variance ratio. Between 10 and 15 mm, the effect of the interaction is reversed. The details of the factor matrix can be found in Equations 5-8.

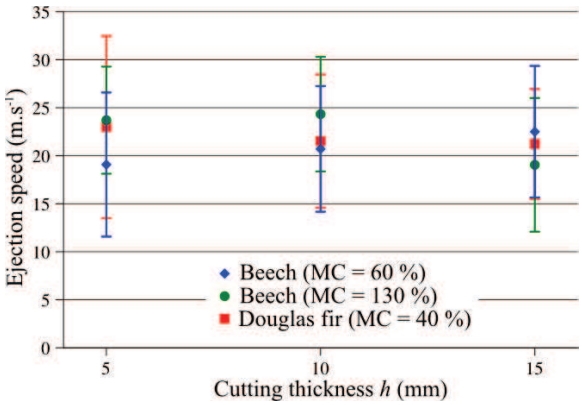


**Figure 7:** Chip ejection speed function of cutting thickness. Mean and standard deviation of 100 values.
($b$ = 10 mm, $GD$ = 90°)

$$M = 21.56 \qquad E_B = [-0.172 \quad 0.957 \quad -0.785]$$

$$E_A = [-0.799 \quad 0.799] \qquad I_{AB} = \begin{bmatrix} -1.512 & 1.512 \\ -1.015 & 1.015 \\ 2.527 & -2.527 \end{bmatrix}$$

**Equations 5-8:** Factor matrix for the chip ejection speed

Concerning the effect of the grain direction angle on chip thickness (Figure 8), it can be observed that the mean chip thickness slightly decreases with GD and reaches a minimum of 10° before the end of the good chipping area.
Finally the ejection speed increases slightly between 70° and 80° (Figure 9). At 90°, it seems that there is a modification of the slope up to 100° where the ejection speed is more than two times higher than at GD = 70°.

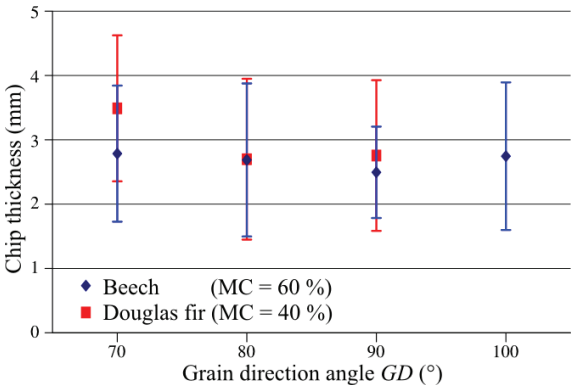


**Figure 8:** Chip thickness function of grain direction angle. Mean and standard deviation of 100 values.
($b$ = 10 mm, $h$ = 10 mm)

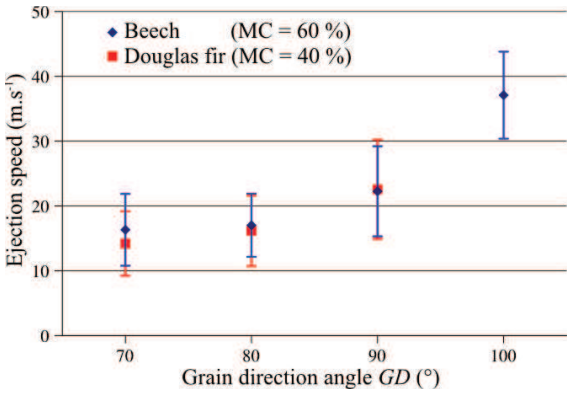


**Figure 9:** Chip ejection speed function of grain direction angle. Mean and standard deviation of 100 values. ($b$ = 10 mm, $h$ = 10 mm)

## Strain and strain-rate fields

Some specimens are painted in white and coated with a speckle pattern in order to observe surface strain and strain rate fields. 7D digital correlation software is used (10). The size of the zone of interest (ZOI) is fixed at 10 pixels. To avoid the appearance of numerical noise a smoothing is

applied with a related length corresponding to one ZOI. This filtering operation induces an underestimation of the strains of 0.1 %.
The maximal resolution of the camera of 512 x 640 pixels at a 20 kHz frame rate represents 44 µm.pixel$^{-1}$ in the surface of the specimen. Due to this scale and the large deformations under the cutting face, we are not able to observe the strain field at the cutting edge. In all directions at least the length of one ZOI is missing.

Figure 10 shows an example of strain field in the cutting direction for beech at *GD* = 90° and *h* = 15 mm. For a better observation, the strain is plotted for some lines of interest under and above the cutting plane.

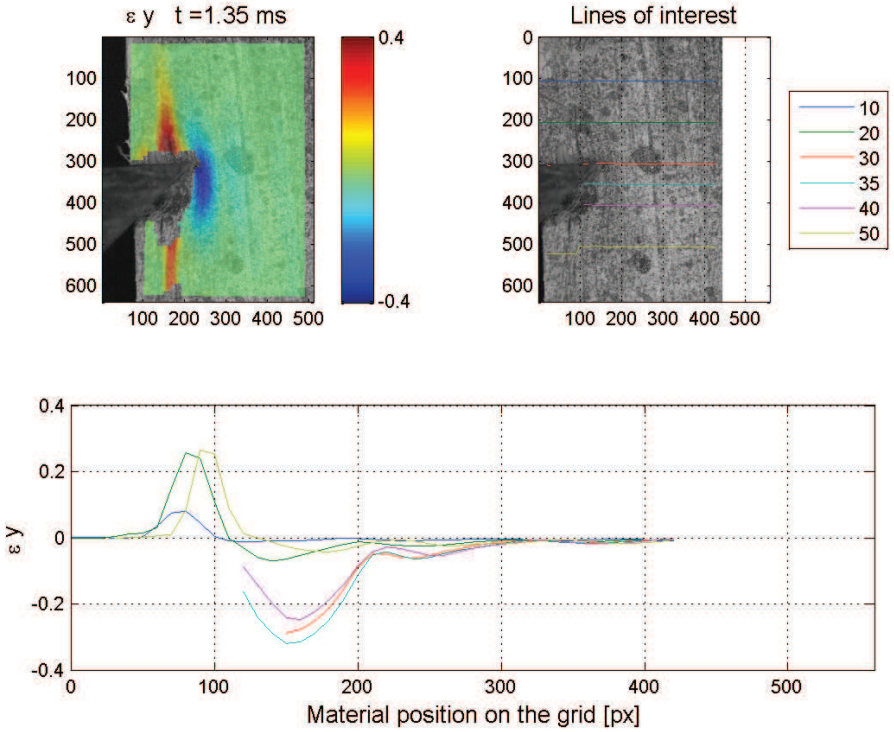


**Figure 10:** Strain field in the cutting direction with detail of the strain field on different lines of interest in the grid. (Beech, *GD* = 90°, *h* = 15 mm, *b* = 10 mm, MC = 60 %).

From Figure 10 we can say that the breakage which creates the chip occurs at the same position as the one above the cutting flank with an uncertainty of one ZOI. In the cutting direction, the material is crushed more than 4 mm above the cutting edge. The DIC software represents the fractures by huge tensile strains (like in pixels 80-100 for the lines 10, 20, 50). These strains are not real.

From these fields it is possible to obtain the maximum strains and strain rates before chipping in all directions (Table 2). These results can be useful to evaluate the performance of the chipping simulations.

| Direction | Strain | | Strain rate | |
|---|---|---|---|---|
| | Under cutting face | Above cutting flank | Under cutting face | Above cutting flank |
| Cutting | -30 to -40 % | Hard to observe | 1000 to 2000 s$^{-1}$ | 1000 to 2000 s$^{-1}$ |
| Feed | Hard to observe | Hard to observe | 500 s$^{-1}$ | 500 s$^{-1}$ |
| Shearing | 10 % | 10 to 20 % | 1000 s$^{-1}$ | 1000 s$^{-1}$ |

**Table 2**: Maximum strains and strain rates obtained before chipping.

## CONCLUSIONS

This study shows that a good chipping area exists and depends on the species, the moisture content and the specimen geometry. At cross grain cutting, chipping does not occur but separation by tearing. Chip thickness increases with cutting thickness but decreases with the grain direction angle and the moisture content. Chip ejection speed highly augments with the grain direction angle at cross grain cutting. Digital image correlation allows the observation of strains and strain rates fields at high cutting speed. These results will be useful to evaluate the performance of the chipping simulations.

### Acknowledgements

This research was carried out at the Laboratoire Bourgogne des Matériaux et des Procédés (LaBoMaP), Ecole Nationale Superieure d'Arts et Métiers (ENSAM), Cluny, Bourgogne, France. We wish to thank our partners and funders of the Xylomat Technical Platform from the Xylomat Scientific Network funded by ANR-10-EQPX-16 XYLOFOREST. We acknowledge LaMCoS laboratory for their technical support in high speed motions; Jean-Claude Butaud, Fabrice Cottin and Roger Letourneau LaBoMaP research engineers and technician; Philippe Lorong and Morgane Pfeiffer-Laplaud for their availability and advice.

## REFERENCES

1. Abdallah R (2010) Détermination des facteurs influençant la coupe et la qualité des plaquettes issues du déchiquetage du bois par des machines forestières. Université de Nancy. PhD Thesis.
2. Felber G, Lackner R (2005) Optimisation of the production of sawmills chips for the pulp and paper industry. In Proceeding IWMS 17, pp 225-240.
3. Hernandez RE, Quiron B (1993) Effect of a chipper-canter knife clamp on the quality of chips produced from black spruce. Forest Products Journal, 43(9): 8-14.
4. Buchanan JG, Duchnicki TS (1963) Some experiments in low-speed chipping. Pulp and Paper Magazine of Canada, 5: 235-245.
5. Hellström L (2010) On the wood chipping process – A study on basic mechanisms in order to optimize chip properties for pulping. Mid Sweden University, Department of Natural Sciences, Engineering and Mathematics. PhD Thesis.
6. Chardin A (1958) Utilisation du pendule dynamométrique dans les recherches sur le sciage des bois tropicaux. Bois et Forêts des Tropiques, 58 : 49-61.
7. Eyma F, Méausoone P, Larricq P, Marchal R (2005) Utilization of a dynamometric pendulum to estimate cutting forces involved during routing. Comparison with actual calculated values. Annals of Forest Science, 62(5): 441-447.
8. Pfeiffer R, Collet R, Denaud LE, Fromentin G (2015) Analysis of chip formation mechanisms and modelling of slabber process. Wood Science and Technology, 49(1): 41-58.
9. ISO 3002-1 (1982) Basic quantities in cutting and grinding. Part 1: Geometry of the active part of cutting tools. General terms, reference systems, tool and working angles, chip breaker.
10. Vacher P, Dumoulin S, Morestin F, Mguil-Touchal S (1999) Bidimensional strain measurement using digital images. Proceedings of the Institution of Mechanical Engineers, Part C: Journal of Mechanical Engineering Science 213(8): 811–817.